Neuromorphic Implementation of Attractor Dynamics in Decision Circuit with NMDARs

Hongzhi You*, Dahui Wang†

*Key Laboratory for NeuroInformation of Ministry of Education, Center for Information in BioMedicine
School of Life Science and Technology, University of Electronic Science and Technology of China, China
† School of Systems Science, State Key Laboratory of Cognitive Neuroscience and Learning, Beijing Normal University, China

Email: hongzhi-you@uestc.edu.cn

***Abstract*—Emulation of decision making in neuromorphic system can be useful for developing remarkable bio-mimetic devices capable of implementing adaptive and interactive behaviors with the varying environment. Both experimental and theoretical studies reveal that the dynamics of NMDA receptors (NMDARs) plays a critical role in attractor dynamics of decision. However, the functionality of NMDARs has not been considered in current neuromorphic decision circuit. Here we present a novel method for the neuromorphic implementation of a two-variable decision circuit with NMDARs. Circuit simulations and theoretical analysis reveal that the decision circuit can present not only the winner-take-all mechanism but also the slow integration of sensory evidences, both of which are embedded in gradually ramp-up activities observed in our simulations and in the electrophysiological recording in monkey's experiments. We demonstrated that the decision circuit we built can generate reliable attractor dynamics capable of reproducing both neurophysiological and behavioral observations during decision tasks.**

I. Introduction

Perceptual decision making is an important cognitive function of selecting an option or an action from among a set of alternatives, and its physical implementation in silicon is of benefit to develop new generation of technologies that carry out brain-like artificial intelligence while maintaining remarkable energy efficiency [1]. Experimental and theoretical researches found that the attractor dynamics of decision making relies on not only the saddle-node structure of the recurrent neural network that achieves the functionality of selecting an alternative, but also the dynamics of NMDA receptors (NMDARs) that contributes to the slow time integration of sensory evidences [2]. Recently, the forced two-choice decision tasks based on the discrete recurrent network was implemented in a custom mixed signal analog/digital neuromorphic chip containing an array of 58 analog integrate-and-fire neurons and programmable synapses [3] . Also these tasks based on the continuous recurrent network was achieved in the integrate-and-fire stop-learning winner-take-all chip [4]. The nonlinear dynamics of the NMDAR-mediated synaptic current is not taken into account in these neuromorphic systems, but saturation characteristics of silicon neurons and AMPA receptor-mediated synaptic currents [5] with the long time constant instead. Although the decision tasks can be implemented in these systems, the range of neural coding by the firing activity in the decision task is narrowed and the slow dynamics for the evidence integration is deteriorated.

In this work, we developed a decision circuit with NMDARs according to the two-variable version of a biophysical plausible decision model proposed by Wong and Wang [6]. In particular, using the dynamic voltage-current circuit and multipliers (Figure 1), we applied the dynamical system approach of circuit synthesis to implement the NMDAR gating variable circuit (Figure 2), which is described by the first order kinetic equation of a reversible chemical reaction. Circuit simulations demonstrated that the NMDAR gating variable circuit can capture the nonlinear dynamical characteristics of corresponding gating variable, and the decision circuit with NMDARs can reproduce ramping neural activities observed in the electrophysiological recording in monkey's experiments [7]. The slope of these activities increases with the coherence of sensory inputs, and the reaction time decreases with the coherence of sensory inputs. Meanwhile, by comparing these simulations with results from the phase-plane analysis for the two-variable decision model, our decision circuit with NMDARs shows neural activities and behaviors predicted by the saddle-node structure during the decision task. Both simulations and theoretical analysis demonstrated that this neuromorphic circuit has attractor dynamics of perceptual decision making.

The paper is organized as follow: first, neuromorphic circuit of the NMDAR gating variable and a two-variable decision model were introduced in the methods section; second, results from circuit simulations and theoretical analysis were shown and demonstrated attractor dynamics of decision can be implemented completely; finally, results were discussed and concluded in the conclusions section.

II. Materials and Methods

A. Neuromorphic circuit of the NMDAR gating variable

Experimental and theoretical researches found that the NMDA receptors at recurrent synapses are important to slow time integration in decision making [6]. The dynamics of the NMDAR gating variable is characterized by a fast rise

978-1-4799-5341-7/16/$31.00 ©2016 IEEE

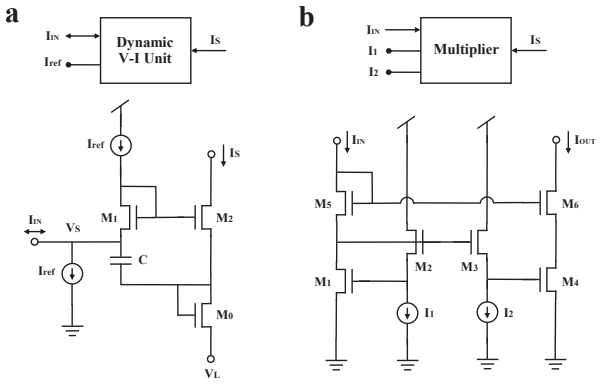

Fig. 1: Schematics of dynamic voltage-current unit (DVI) and multiplier (M).

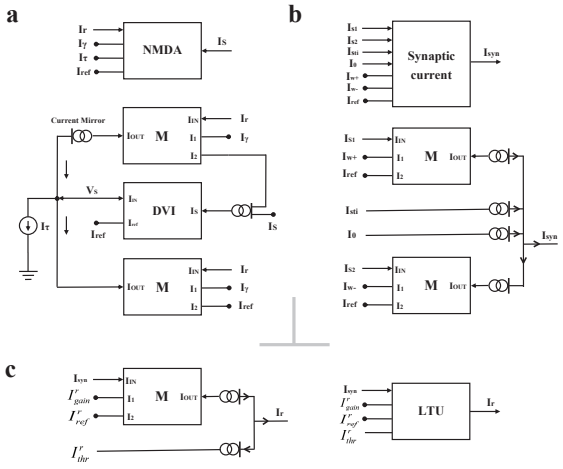

Fig. 2: The block representations of the NMDAR gating variable circuit (a), the synaptic current circuit (b) and the linear threshold unit circuit (c).

followed by a slow decay. When the presynaptic inputs at recurrent synapse in a neural population are described by a Poisson spike train at a rate of r per cell, the slow dynamics of the average NMDAR gating variable S is characterized by the nonlinear differential equation as follows:

$$\frac{dS}{dt} = -\frac{S}{\tau} + (1-S)\gamma r \tag{1}$$

where τ is the decay time constant, and γ is a gain cofficient. In order to implement the circuit of NMDAR gating variable, the corresponding mathematical expression is approximately transformed into the following current-mode description:

$$CU_T \frac{d}{dt}\frac{I_S}{I_{ref}} = -I_\tau \frac{I_S}{I_{ref}} + (1 - \frac{I_S}{I_{ref}})\frac{I_\gamma}{I_{ref}} I_r \tag{2}$$

where dimensionless variables S and γ are replaced by two ratios of currents $\frac{I_S}{I_{ref}}$ and $\frac{I_\gamma}{I_{ref}}$, respectively. I_r is a current representing r, and the time constant $\tau = \frac{CU_T}{I_\tau}$. Equation 1 and Equation 2 are not rigorously equivalent, but have similar dynamics.

We used a dynamic voltage-current circuit (DVI) originally proposed for the log-domain circuit [8] to achieve the derivative on the left side of Equation 2 (Figure 1a). Since

$$\frac{I_S}{I_{ref}} = \frac{I_{M_2}}{I_{M_1}} = e^{\frac{V_S - V_0}{U_T}} \tag{3}$$

the dynamics of the voltage difference $V_S - V_0$ has the following relationship with I_S/I_{ref}:

$$\frac{d}{dt}\frac{I_S}{I_{ref}} = \frac{1}{U_T}\frac{I_S}{I_{ref}}\frac{d}{dt}(V_S - V_0) \tag{4}$$

By combining Equation 4 and Equation 2, we can get the following voltage-mode differential equation to characterize the dynamics of S:

$$C\frac{d}{dt}(V_S - V_0) = -I_\tau + \frac{I_\gamma}{I_S} I_r - \frac{I_\gamma}{I_{ref}} I_r \tag{5}$$

According to the dynamical systems approach of circuit synthesis [9], we require three currents to drive the capacitor in the dynamic voltage-current circuit (Figure 1a and Figure 2) to realize the circuit: two currents decrease the capacitor voltage and one increases it. The first current term I_τ corresponds to the time constant of the circuit. The second term and the third term can be generated by using a multiplier (Figure 1b and Figure 2a) on the basis of the translinear principle for subthreshold transistors [10], [11].

B. Neuromorphic implementation for a firing rate model of decision making

In the two-variable decision model developed by Wong and Wang [6], two dynamical variables S_1 and S_2 represent averaged gating variables of two populations selective for rightward and leftward motion directions. For the sake of neuromorphic implementations, original reduced model is re-expressed in the current-mode description. First, we have a two-variable systems described by the following dynamical equations (also same with Equation 2):

$$CU_T \frac{d}{dt}\frac{I_{S,i}}{I_{ref}} = -I_\tau \frac{I_{S,i}}{I_{ref}} + (1 - \frac{I_{S,i}}{I_{ref}})\frac{I_\gamma}{I_{ref}} I_{r,i} \tag{6}$$

in which i $(= 1,2)$ labels two selective populations. For the sake of simplicity, we adopted the linear-threshold unit (LTU) to model the firing rates of two populations $I_{r,i}$, which are given by the equation as follows:

$$I_{r,i} = [\frac{I^r_{gain}}{I^r_{ref}} I_{syn,i} - I^r_{thr}]^+ \tag{7}$$

where the dimensionless variable $\frac{I^r_{gain}}{I^r_{ref}}$ is the gain of the neural population and $\frac{I^r_{ref}}{I^r_{gain}} I^r_{thr}$ is the threshold current. $I_{syn,i}$ denotes corresponding synaptic current. $[x]^+$ is equivalent to the function $max(x,0)$. According to Equation 7, we only require a multiplier and several current mirrors to realized the LTU circuit (Figure 2c). In the phase-plane analysis (Figure 4c), we used Equation 8 as the model of the LTU circuit

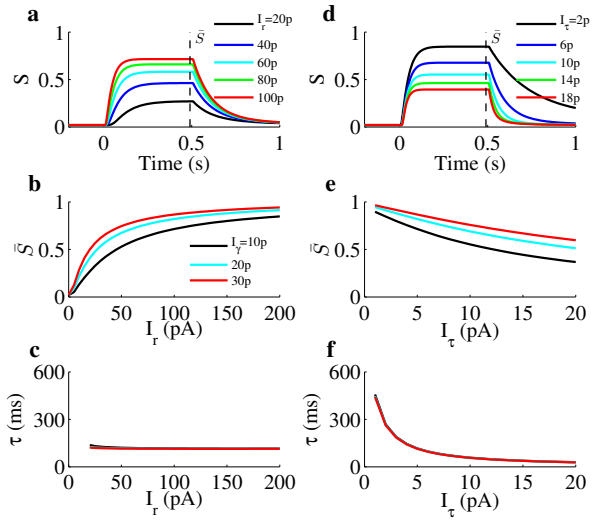

Fig. 3: **Characteristics of the NMDAR gating variable circuit. (a)** Transient responses in circuit simulations for varying firing rate I_r. The gating variable $S = I_S/I_{ref}$. I_r is presented during the first $0.5s$. The dashed vertical line indicates the state $\bar{S}$, in which the state of the circuit becomes stable. Parameters: $I_\gamma = 10pA$, $I_\tau = 5pA$ and $I_{ref} = 100pA$. **(b)** $\bar{S}$ increases with I_r and I_γ. Figure b,c,e and f have a unified legend. **(c)** Time constant of the circuit τ is independent of I_r and I_γ. The errors of τ for small I_r and I_γ are derived from the decreasing of the effective I_τ that is copied from a current mirror. **(d)** Transient responses in circuit simulations for varying current I_τ. Parameters: $I_r = 100pA$, $I_\gamma = 10pA$ and $I_{ref} = 100pA$. **(e)** $\bar{S}$ decreases with I_τ. **(f)** The time constant of the circuit τ decreases with I_τ, but is independent of I_γ.

instead of Equation 7:

$$I_{r,i} = \left(\frac{I^r_{gain}}{I^r_{ref}} I_{syn,i} - I^r_{thr}\right)/\left(1 - \exp\left(-g\left(\frac{I^r_{gain}}{I^r_{ref}} I_{syn,i} - I^r_{thr}\right)\right)\right) \quad (8)$$

in which the parameter g tunes the smoothness of the firing rate curve around the threshold current. The total synaptic currents of two selective populations $I_{syn,i}$ are given by following equations, respectively:

$$\begin{cases} I_{syn,1} = I_{w^+}\frac{I_{S,1}}{I_{ref}} - I_{w^-}\frac{I_{S,2}}{I_{ref}} + I_0 + I_{sti,1} \\ I_{syn,2} = I_{w^+}\frac{I_{S,2}}{I_{ref}} - I_{w^-}\frac{I_{S,1}}{I_{ref}} + I_0 + I_{sti,2} \end{cases} \quad (9)$$

in which $I_{sti,i}$ represents the external motion stimulus to the population i and I_0 is the effective background input. $I_{sti,1} = I_{sti}(1+coh)$, and $I_{sti,2} = I_{sti}(1-coh)$, in which I_{sti} denotes the stimulus strength and coh denotes the coherence level of the stimulus. I_{w^+} and I_{w^-} are effective self-excitation and mutual-inhibition current per unit (the gating variable) in the recurrent network, respectively. The synaptic current block can also be realized by two multipliers and several current mirrors (Figure 2b).

III. Results

A. Dynamic characteristics of the NMDAR gating variable circuit

We built the neuromorphic circuit of the NMDAR gating variable by using one dynamic voltage-current uint (DVI), two multipliers and several current mirrors according to Equation 5 (Figure 2a). Major dynamic characteristics of this circuit we concentrated on are the steady state and the time constant for a given configuration. From Equation 2, we can get the steady state $\bar{S}$ and the time constant τ as follows:

$$\bar{S} = \frac{\frac{I_\gamma}{I_{ref}} I_r}{I_\tau + \frac{I_\gamma}{I_{ref}} I_r}, \tau = \frac{CU_T}{I_\tau} \quad (10)$$

We initially test the response of this gating variable circuit through simulation with the constant stimulus (I_r) presented during the first 0.5s(Figure 3). Before the stimulus onset, the gating variable S stays at a low state. Once the stimulus are presented, the gating variable increases gradually and then keeps in its steady state. The steady state $\bar{S}$ increases with the input current I_r, but decreases with the current I_τ (Figure 3a,b,d,e). Meanwhile, $\bar{S}$ is also dependent on the gain current I_γ, which determines the gain cofficient of the circuit. Larger gain current I_γ leads to higher steady state $\bar{S}$ and more distinct nonlinear saturation characteristics (Figure 3b). These simulation results are consistent with predictions from Equation 10. After the offset of the stimulus, the gating variable S decays exponentially, and the corresponding decay speed increases with the current I_τ (Figure 3d). Meanwhile, the decay response after the cancellation of the stimulus I_r shows that the time constant τ decreases with the current I_τ and is independent on I_r and I_γ (Figure 3c and f), which are also consistent with the conclusion from Equation 10. Simulation results demonstrated that the NMDAR gating variable circuit we built can implement the major dynamics of its biological counterpart.

B. Emulation of decision and its attractor dynamics in the decision circuit with NMDARs

According to Equation 6,7 and 9, we built the neuromorphic circuit of decision making, the block representation of which is not shown here for lack of space in this paper but follows the similar assembling principle as Figure 2.

We tested responses of this decision circuit through simulations by the stimulus with different coherence levels, which are given after $0s$ (Figure 4a). Responses of both populations stay at a low activity before the stimulus onset. After the stimulus is presented, one of them has a gradually ramp-up activity and the other has a gradually decreasing activity. According to the decision bound theory supported by some observations in the monkey experiment [12], we set a fixed firing rate as the decision threshold in our circuit simulations. Decision is made once the activity of any population exceeds the decision threshold, and corresponding time is measured as the reaction time. The speed of the ramp-up activity increases with the coherence of the stimulus, and the reaction time decreases with it (Figure 4b), both of which are consistent with neural activities and behaviors observed in the monkey experiments, respectively [7]. However, because our decision circuit is a noise-free system, the reaction time has a linear relationship

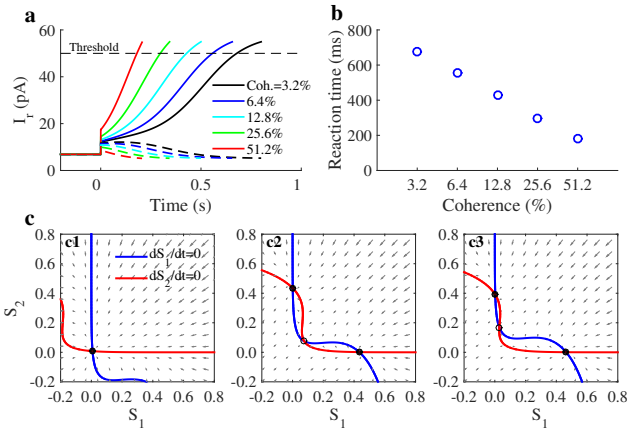

Fig. 4: **Decision making and its attractor dynamics in the neuromorphic decision circuit. (a)** Firing activities in the decision task. The stimuli are presented to the circuit after 0s. Colors indicate different coherence levels of the stimuli. **(b)** The decision time decreases as the coherence level increases. **(c)** Phase-plane plot for two neural populations in the decision task, without external input (**c1**), in the presence of unbiased stimuli (**c2**:$Coh. = 0\%$) or biased stimuli (**c3**:$Coh. = 12.8\%$). $I_{sti} = 15pA$. Solid dots denote stable steady states, and circles denote unstable steady states.

with the logarithm of the coherence level (Figure 4b), which has been observed in previous studies [4].

These simulation results can be interpreted by a phase-plane analysis of the model described by Equation 6,7 and 9 (Figure 4c). In the (S_1,S_2) phase space (decision space), two lines called nullclines are plotted first by setting the dynamical equations $dS_1/dt = 0$ and $dS_2/dt = 0$ (Equation 6), respectively. The intersections of two nullclines are steady states of the model. Meanwhile, the direction field in the phase space shows how the system state will evolve. In the absence of a stimulus, the two nullclines intersect with each other only once, producing a stable steady state, that is, an attractor (Figure 4c1), which explains that two populations in the decision circuit have low spontaneous activities before the stimulus onset. When an unbiased stimulus is presented ($Coh. = 0\%$), two nullclines intersect with each other three times and produce a saddle-type unstable and two stable steady states(Figure 4c2). They form two basins of attraction around two attractors, respectively, representing two alternatives in the decision. The system state locates in the vicinity of the unstable steady state before the stimulus onset, and then evolves toward one of two attractors once the stimulus is onset. This saddle node structure determines the time course of neural activities underlying two-alternative decision. When a biased stimulus is applied, the phase space is no longer symmetrical. As an example of the biased stimulus $Coh. = 12.8\%$ (Figure 4c3), the unstable steady state is closer to the attractor that represents the second alternative, the fact of which shows that the attractor state responsible to the first alternative has a larger basin of attraction than the other. At the onset of a biased stimulus, the initial state of the system is already lies within the basin of the attractor of the first alternative, and the system state will evolve toward its favored attractor, especially for our noise-free circuit.

IV. Conclusions

In this study, we constructed a two-variable neuromorphic decision circuit with the functionality of NMDARs to implement the attractor dynamics of perceptual decision making. We demonstrated that this circuit presents both winner-take-all behavior and gradually ramp-up activities, which are determined by the saddle-node structure in the dynamics and the slow integration of sensory evidences, respectively. Moreover, the nonlinear dynamics of the NMDAR-mediated synaptic current contributes to the improvement of neural coding by the firing activity during the decision task. The theoretical and emulation results in this study are important for the embodiment of our decision circuit on the hardware in the next step. A reliable decision module, as well as neuromorphic modules with other coginitive functions already developed, such as working memory [13] and synaptic plasticity [14], [15], are critical to the framework of the neuromorphic cognitve system.

Acknowledgment

This work has been supported by NSFC under grants 31500863, 31271169 and the 973 project 2013CB329401.

References

[1] G. Indiveri and T. K. Horiuchi, "Frontiers in neuromorphic engineering," *Frontiers in neuroscience*, vol. 5, 2011.
[2] X.-J. Wang, "Probabilistic decision making by slow reverberation in cortical circuits," *Neuron*, vol. 36, no. 5, pp. 955–968, 2002.
[3] F. Corradi, *et al.*, "Decision making and perceptual bistability in spike-based neuromorphic vlsi systems," pp. 2708–2711, 2015.
[4] H. You, "Neural dynamics of perceptual decision making and its emulation on neuromorphic chip," *Phd thesis, Beijing Normal University*, 2014.
[5] C. Bartolozzi and G. Indiveri, "Synaptic dynamics in analog vlsi," *Neural computation*, vol. 19, no. 10, pp. 2581–2603, 2007.
[6] K.-F. Wong and X.-J. Wang, "A recurrent network mechanism of time integration in perceptual decisions," *The Journal of neuroscience*, vol. 26, no. 4, pp. 1314–1328, 2006.
[7] M. N. Shadlen and W. T. Newsome, "Neural basis of a perceptual decision in the parietal cortex (area lip) of the rhesus monkey," *Journal of neurophysiology*, vol. 86, no. 4, pp. 1916–1936, 2001.
[8] T. Yu and G. Cauwenberghs, "Analog vlsi biophysical neurons and synapses with programmable membrane channel kinetics," *Biomedical Circuits and Systems, IEEE Transactions on*, vol. 4, no. 3, pp. 139–148, 2010.
[9] J. V. Arthur and K. Boahen, "Silicon-neuron design: A dynamical systems approach," *Circuits and Systems I: Regular Papers, IEEE Transactions on*, vol. 58, no. 5, pp. 1034–1043, 2011.
[10] B. Gilbert, "Translinear circuits: A proposed classification," *Electronics Letters*, vol. 11, no. 1, pp. 14–16, 1975.
[11] K. I. Papadimitriou, *et al.*, "Systematic computation of nonlinear cellular and molecular dynamics with low-power cytomimetic circuits: a simulation study," *PloS one*, vol. 8, no. 2, p. e53591, 2013.
[12] R. Kiani, *et al.*, "Bounded integration in parietal cortex underlies decisions even when viewing duration is dictated by the environment," *The Journal of Neuroscience*, vol. 28, no. 12, pp. 3017–3029, 2008.
[13] M. Giulioni, *et al.*, "Robust working memory in an asynchronously spiking neural network realized with neuromorphic vlsi," *Frontiers in neuroscience*, vol. 5, 2011.
[14] S. Fusi, *et al.*, "Spike-driven synaptic plasticity: theory, simulation, vlsi implementation," *Neural computation*, vol. 12, no. 10, pp. 2227–2258, 2000.
[15] G. Indiveri, *et al.*, "Spike-based learning with a generalized integrate and fire silicon neuron," in *Circuits and Systems (ISCAS), Proceedings of 2010 IEEE International Symposium on*. IEEE, 2010, pp. 1951–1954.